Available online at www.sciencedirect.com
SCIENCE DIRECT®

Journal of the European Ceramic Society 24 (2004) 2853–2860
www.elsevier.com/locate/jeurceramsoc

Study on the stability of Ce α-Sialon derived from SHS-ed powder

Jiuxin Jiang[a], Peiling Wang[a,*], Wanbao He[b], Weiwu Chen[a], Hanrui Zhuang[b], Yibing Cheng[c], Dongsheng Yan[a]

[a]*The State Key Lab of High Performance Ceramics and Superfine Microstructure, Shanghai Institute of Ceramics, Chinese Academy of Science, Shanghai 200050, PR China*
[b]*The Center of Structural Ceramics, Shanghai Institute of Ceramics, Chinese Academy of Science, Shanghai 200050, PR China*
[c]*School of Physics and Materials Engineering, Monash University, Clayton, Victoria 3800, Australia*

Received 12 June 2003; received in revised form 8 September 2003; accepted 20 September 2003

Abstract

The synthesis of Ce α-Sialon powder by self-propagating high-temperature synthesis (SHS) and the sintering behaviors of Ce α-Sialon material by hot-pressing derived from SHS-ed powder with the addition of CeO_2 or Y_2O_3 were performed in the present work. The results have shown that the phase assemblages of synthesized Ce α-Sialon powder consisted of β-Sialon, as the major crystalline phase, and small amount of α-Sialon, $Ce_2Si_6O_3N_8$ and AlN-polytypoid. Ce α-Sialon phase was meta-stable and would decompose to β-Sialon and JEM phase [$Ce(Si_{6-z}Al_z)(N_{10-z}O_z, z\approx1)$] with the disappearance of $Ce_2Si_6O_3N_8$ and AlN-polytypoid after hot-pressing. The addition of CeO_2 further encouraged the transformation of Ce α-Sialon phase, but the addition of Y_2O_3 did stabilize the Ce α-Sialon structure and (Ce,Y) α-Sialon phase would be as the major crystalline phase in the sintered material when 0.375 molar Y_2O_3 was added, in which most α-Sialon grains having elongated morphology were observed. As a result, the hardness (H_v) and fracture toughness (K_{IC}) of sintered (Ce,Y) α-Sialon material being 15.23 GPa and 4.90 MPa $m^{1/2}$ respectively were obtained.

Keywords: Hot pressing; Mechanical properties; Phase stability; SHS; Sialons

1. Introduction

Si_3N_4-based ceramics are the promising candidates at high temperature and corrosive environments in the metallurgy and chemical industries, due to their outstanding properties of super-wear, corrosion resistance, good anti-oxidation and thermal shock behavior, as well as high strength and hardness up to high temperature.[1] Sialons, the solid solution of Si_3N_4, have two modifiers, i.e. α-Sialon and β-Sialon (abbreviated as α′ and β′, respectively), represented by the formula of $M_xSi_{12-(m+n)}Al_{(m+n)}O_nN_{16-n}$ and $Si_{6-z}Al_zO_zN_{8-z}$ respectively, where m(Si-N) are substituted by m(Al-N) and n(Si-N) by n(Al-O) in α′, and z(Si-N) by z(Al-O) in β′, and the valence discrepancy introduced in α′ is counterbalanced by some metal cations. In conventional synthesis methods, these cations include Li^+, Mg^{2+}, Ca^{2+}, Y^{3+} and some lanthanides ions with exception of Ce^{3+}, Pr^{3+} and Eu^{3+}.[2,3] However, attention to α′ stabilized by rare earth ions that could not be absorbed into α′ structure by conventional synthesis, such as Ce^{3+}, has been paid in the last two decades. [4–11] Studies by Ekström and co-workers on the sintering of Sialon ceramics showed that a small amount of cerium ions can be incorporated into the large interstitial holes of α′ structure if yttrium is added as additive simultaneously.[4,5] This observation has also been confirmed by a high-resolution electron microscopy study by Olsson.[6] However, the same authors [4] claimed that Ce could not enter Sialon structure if CeO_2 alone is used as the sintering additive. Later, researches by Mandal and co-workers indicated that certain α′ rich compositions are greatly affected by post-sintering cooling rate so that the amount of α′ significantly increases if the samples are fast cooled.[7] This result can be well interpreted by the theory proposed by Rosenflanz and Chen[8] and by Shen,[9] i.e. α′ phase may persist as a meta-stable phase only in systems where thermodynamic equilibrium varies with temperature and when the true thermodynamic equilibrium is kinetically retarded. This approach opens up another route for producing α′ containing large size

* Corresponding author.
E-mail address: plwang@sunm.shcnc.ac.cn (P. Wang).

0955-2219/$ - see front matter © 2003 Elsevier Ltd. All rights reserved.
doi:10.1016/j.jeurceramsoc.2003.09.005

ions such as Ce^{3+}. Recent study by Wang et al.[10] manifested that plasma-activated sintering (PAS) can be used for the synthesis of Ce α′, but with the precondition of the addition of 1 wt.% Y α′ powder as nuclei. They suggested that the formation of Ce α′ is controlled by the nucleation at the surface of α′ nuclei. However, investigation by Shen and co-workers[11] on Ce α′ materials fabricated by spark plasma sintering (SPS, similar to PAS) showed that α′ is the major crystalline phase in the sintered compact, which contrasts against previous conclusions that Ce could not enter the α′ structure if CeO_2/Ce_2O_3 is alone used as the sintering additive. They proposed that the very rapid heating and cooling process contribute to the formation of Ce α′ and the products are meta-stable.

Self-propagating high-temperature synthesis (SHS) has been considered to be a promising technique for the synthesis of advanced materials,[12–14] such as carbide, nitride, boride and $MoSi_2$. High reaction temperature, rapid reaction rate and low costs are the special advantages of the synthesis technology. The process becomes self-sustaining once the reactant are ignited, the temperature can reach thousands degrees in seconds and the reaction can be completed in seconds, moreover, the process dose not require complex high-temperature device. This technique has been used for the disposal of industrial wastes recently.[15] The similarity of rapid reaction between SHS and SPS techniques has prompted the present study on the SHS synthesis of α′ stabilized by Ce, which could not enter the α′ structure by conventional synthesis methods. In our previous work, the synthesis of (Ca,Mg) α′ powder using SHS technique[15] and the formation behavior of SHS-ed (Ca,Mg) α′ ceramics[16] have been reported. The results showed that SHS-ed (Ca,Mg) α′ phase would decompose to β′ during hot-pressing at 1500 °C and above. However, the addition of extra Ca^{2+} into the SHS-ed α′ powder could improve the stability of the α′ phase. Therefore, the synthesis of Ce α′ powders by SHS and study on the stability of Ce α′ after hot-pressing without and the addition of CeO_2 or Y_2O_3 using SHS-ed Ce α′ composition as the starting material is worthy. It will be especially interesting to compare the difference in stability of SHS-ed α′, which are stabilized by Ce, not forming α′ by conventional method, and Ca, having highest solid solution range in α′. In addition, if the transformation of α′ to β′ phase would happen during hot-pressing in Ce α′ system as that in (Ca,Mg) α′ case, the microstructure of Ce α′ material could be modified and hence its mechanical properties could be tailored.

2. Experimental

The starting powders used are Si_3N_4 (UBE E10, Japan, 2 wt.%O), AlN (Wuxi, China, 1.3 wt.%O), CeO_2 (99.99%), Y_2O_3 (99.9%), Si (98%, 30 μm) and Al (98%, 25 μm). The nominal composition of Ce α′ designed for SHS lies on the tie line Si_3N_4–9AlN:Ce_2O_3, corresponding to the composition of $x=0.5$, $m=1.5$ and $n=0.75$, i.e. $Ce_{0.5}Si_{9.75}Al_{2.25}O_{0.75}N_{15.25}$. The compositions used for hot-pressing without and with addition of CeO_2 or Y_2O_3 are listed in Table 1. The corresponding samples are symbolized as Ce1, Ce4Ce1, Ce8Y1, Ce8Y2 and Ce8Y3, respectively.

The mixture powders were put into a graphite crucible and covered with a top layer of titanium powder. A tungsten heating coil was connected to ignite the Ti powder, which then induced the spontaneous SHS process. The detail of the process is the same as described in our previous paper.[15]

The synthesized powders were attrition milled for 24 h and then were hot-pressed in flowing N_2 at 1750 °C for 1h under the pressure of 20 MPa in a graphite furnace. Mixtures of SHS-ed Ce α′ composition and CeO_2 or Y_2O_3 were well mixed in agate mortar for 2 h, dried under the infrared lamp and then were hot-pressed under the same condition as the sample without addition of CeO_2 or Y_2O_3.

The bulk densities of samples were measured according to the Archimedes principle. Phase assemblages of the powders and sintered samples were determined on the base of X-ray diffraction data from a Guinier-Hägg camera with use of Cu $K_{\alpha1}$ radiation and Si as an internal standard. The measurement of X-ray film and refinement of lattice parameters were completed by a computer-linked line scanner (LS-18) system[17] and SCANPI, PIRUM programs.[18] The semi-quantitative analysis of phase assemblages was carried out on the crystalline content based on the calibration curves. The microstructures observation of hot-pressed α′ samples were performed on SEM (EPMA-8705) equipped with EDS(Oxford/Inca) under backscattered electrons, respectively. To analyze the composition of α′, an average of measurement of three points on different large α′ grains was used as a representative value of EDS analysis for the sample. The hardness and indentation fracture toughness on the hot-pressed samples were measured using a Vickers diamond indenter under a load of 98N.

Table 1
Compositions for hot-pressing samples

Sample symbol	SHS-ed Ce α′ powder : CeO_2 : Y_2O_3	
	Molar ratio	Weight ratio
Ce1	1:0:0	1:0:0
Ce4Ce1	1:0.25:0	1:0.10:0
Ce8Y1	1:0:0.125	1:0:0.045
Ce8Y2	1:0:0.250	1:0:0.090
Ce8Y3	1:0:0.375	1:0:0.134

3. Results and discussion

3.1. Characteristics of SHS-ed Ce α′ powder and hot-pressed material

The XRD pattern of SHS-ed Ce α′ composition is shown in Fig. 1. It was found from XRD results that the major crystalline phase was β′, and the phase assemblages also contained small amount of α′, $Ce_2Si_6O_3N_8$ and AlN-ploytypoid. The weight ratio of α′ to (α′ + β′) in the SHS-ed powders was about 16%, much less than that of (Ca,Mg) α′ formed by SHS.[15]

SHS is a rapid reaction process, and the reaction speed may have the similarity to SPS. However, the result that the amount of Ce α′ phase formed by SHS in the present work is much less than that by SPS [11] may imply that the stability of Ce α′ phase depends not only on the reaction and cooling rate during sintering, but also on whether or not a thermodynamically stable nitrogen-rich Ce^{3+}-containing phase existing, such as $Ce_2Si_6O_3N_8$, whose composition is close to the Ce-doped α′ phase.[11]

The XRD pattern and the phase assemblages of hot-pressed Ce α′ sample Ce1 as well as the cell dimensions of Ce α′ phase are shown and listed in Fig. 2 (a) and Table 2 respectively. It was found that SHS-ed Ce α′ phase would decompose to β′, same as SHS-ed (Ca,Mg) α′ did,[15] during hot-pressing, thus resulting in the decrease of weight ratio of α′ to (α′ + β′) from 16% in the SHS-ed powder to 6% in Ce1 sample. On the other hand, JEM phase ($Ce(Si_{6-z}Al_z)(N_{10-z}O_z)$, $z \approx 1$) appeared as grain boundary phase with higher amount than that of Ce α′ phase in the sintered sample. $Ce_2Si_6O_3N_8$ and AlN-polytypoid phases disappeared at the same time.

As mentioned above that SHS is a very rapid process since reaction temperature could reach as high as above 2000 °C and reaction could be completed within seconds. It is thought that synthesis of α′ by SHS under a high nitrogen pressure is a complex process and the thermodynamic equilibrium is not really achieved in SHS process and the products might be meta-stable. When the SHS-ed powders were reheated to high temperature by hot-pressing, α′ phase would react through liquid phase formed during sintering as follows:

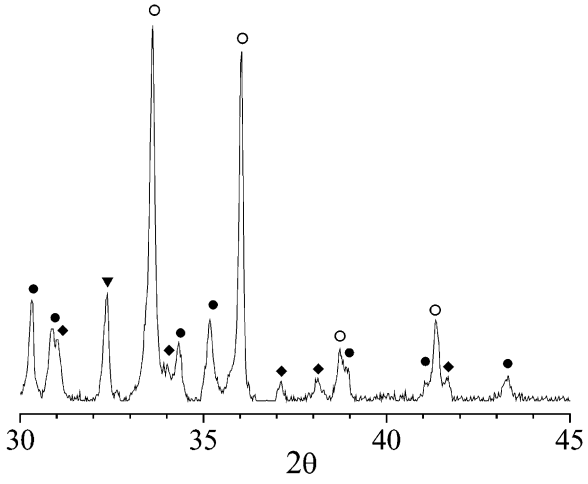

Fig. 1. XRD pattern of Ce α-Sialon powders synthesized by SHS (note: ●, α′; ○, β′; ◆, $Ce_2Si_6O_3N_8$; ▼, AlN-polytypoid).

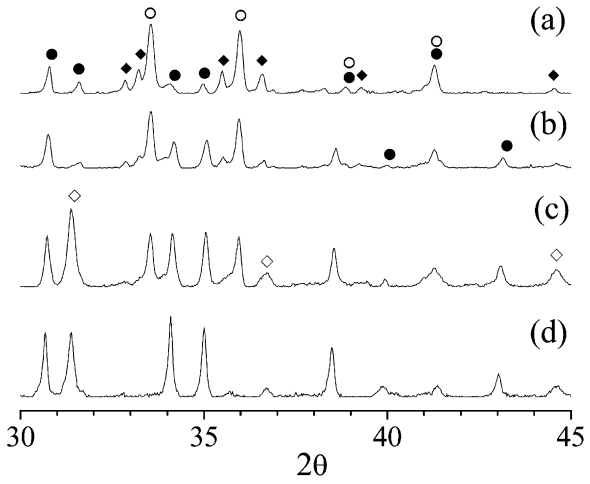

Fig. 2. XRD patterns of hot-pressed Ce α′ samples (a) Ce1 (b) Ce8Y1 (c) Ce8Y2 (d) Ce8Y3 (note: ●, α′; ○, β′; ◆, JEM phase; ◇, M′).

Table 2
Phase assemblages and cell dimensions of α′ in hot-pressed Ce α′ samples

Sample	Phase assemblage[a]	α′/β′	Cell dimensions of α′		Bulk density/g·cm^{-3}
			a(Å)	c(Å)	
SHS-ed Ce α′ powder	β′/s, α′/mw, $Ce_2Si_6O_3N_8$/w, AlN′/w	16/84	7.800(3)	5.670(3)	–
Ce1	β′/s, JEM/mw, α′/w	6/94	7.833(2)	5.707(2)	3.43
Ce 4Ce1	β′/s, JEM/m, α′/tr	≈0	–	–	–
Ce8Y1	β′/s, α′/m, JEM/w	25/75	7.805(1)	5.683(1)	3.44
Ce8Y2	α′/s, β′/ms, M′/m	36/64	7.809(1)	5.692(1)	3.55
Ce8Y3	α′/s, M′/mw	100/0	7.817(1)	5.696(1)	3.61

[a] α′ = α-Sialon; β′ = β-Sialon; M′ = melilite solidation phase; AlN′ = AlN-polytypoid; JEM = $Ce(Si_{6-z}Al_z)(N_{10-z}O_z)$, $z \approx 1$; s = strong; ms = medium strong; m = medium; mw = medium weak; w = weak; tr = trace.

$$\beta'_1 + \alpha'_1 + Ce_2Si_6O_3N_8 + AlN - \text{polytypoid} + \text{liquid}_1 \rightarrow \beta'_2 + \alpha'_2 + \text{JEM} + \text{liquid}_2 \quad (1)$$

Through the transformation of part α′ phase to β′ phase and the new thermodynamic equilibrium in the whole process, some Ce^{3+} ions de-dissolve from α′ structure to grains boundary, forming a thermodynamically more stable phase, i.e. JEM phase. The decrease in the amount of α′ phase after hot-pressing indicated that the Ce^{3+} ions consolidated in the α′ structure by SHS de-dissolved into glass phase or/and the second crystalline phase, i.e. JEM phase. The disappearance of $Ce_2Si_6O_3N_8$ phase and the formation of JEM phase after sintering decreased the Ce/Si ratio of the second phases, resulting in another source of Ce^{3+} ions to be released from grain-boundary phase. It is thought that these Ce^{3+} ions could enter α′ phase that does not decompose, and cause the expanded cell dimensions of α′ phase in hot-pressed Ce1 sample.

3.2. Hot-pressing of Ce α′ powders with the addition of CeO_2/Ce_2O_3

Our previous study[16] on the sintering behaviors of SHS-ed (Ca,Mg) α′ powder showed that the addition of CaO can restrain the phase transformation of α′ to β′ when (Ca.Mg) α′ powder is hot-pressed. However, as shown in Table 2, the addition of CeO_2 in SHS-ed Ce α′ powder did not have the same effect as CaO for SHS-ed (Ca,Mg) α′ powder. The increase in amount of JEM phase and decrease in amount of α′ phase indicated the CeO_2 added do form JEM instead of entering α′ structure and proved that Ce ions can not be incorporated into Sialon structure by conventional process, even the SHS-ed meta-stable Ce α′ powder was used as the starting material.

3.3. Hot-pressing of Ce α′ powders with the addition of Y_2O_3

The XRD patterns and phase assemblages of hot-pressed Ce α′ with the addition of different amounts of Y_2O_3 are shown in Fig. 2(b)–(d) and Table 2, respectively. It was found that the amount of α′ phase increased with increase in the addition of Y_2O_3. The amount of β′ phase decreased while more Y_2O_3 were added. Finally, β′ phase was disappeared when molar ratio of SHS-ed Ce α′ to Y in the nominal composition reached to be 1:0.375 (Ce8Y3 sample). The grain boundary phase varied from JEM phase to M′ (solid solution of N-containing melillite) phase when added Y_2O_3 to SHS-ed powder was increased as 0.25:1.

As mentioned above, the SHS-ed Ce α′ powder is meta-stable, reacted with liquid phase and transformed to β′ when it was sintered at high temperature. When Y_2O_3 was added, Ce α′ powder reacts with Y_2O_3 and liquid phase as following reaction:

$$\beta'_1 + \alpha'_1 + Ce_2Si_6O_3N_8 + AlN + Y_2O_3 + \text{liquid}_1 \rightarrow \beta'_2 + (Ce, Y)\alpha' + \text{JEM} + \text{liquid}_2 \quad (2)$$

It was noted that when small amount of Y_2O_3 was added into SHS-ed α′ powder for sintering as the case of Ce1Y1, the grain boundary in the material was JEM phase, which would be easily formed for Ce-containing composition.[11] Further increasing in the amount of Y_2O_3 in the composition resulted in the formation of M′ phase as the grain boundary phase of the material. The slightly decrease in amount of M′ phase from Ce8Y2 to Ce8Y3 might be attributed to remarked increase of the amount of α′ phase in the later sample. The increase in the cell dimensions of α′ phase resulted from the movement of Ce^{3+} and Y^{3+} during sintering process, i.e. Ce^{3+} ions would redistribute in α′ phase, part of Ce^{3+} ions releasing from remained α′ phase and dissolving into new formed α′ phase, and more Y^{3+} ions would be incorporated into α′ when the amount of α′ phase increased at the same time with more Y_2O_3 added. The bigger cell dimensions of α′ in Ce8Y3 than that in Ce8Y2 do agree with the XRD results of decrease in amount of M′ in Ce8Y3.

The increased bulk densities of sintered samples, as listed in Table 2, were resulted from the increased amount of addition of Y_2O_3 in the compositions.

Some investigations dealing with dual cations α′ have been reported since 1991.[19–21] In these studies, the metal cations which form single-cation α′ exist in any mixed manner to form multi-cation α′ and certain metal cations, such as Ce, Sr, which do not form a single-cation α′, enter the α′ lattice when present in conjunction with other cations, like Y and Ca, that are used as the main stabilizer. In contrast, SHS-ed Ce α′ composition was used as the main starting material for sintering of the ceramics in the present work. It is interesting to see that α′ phase could be obtained as the major crystalline phase in the ceramics by addition of certain amount of Y_2O_3, in which α′ phase was stabilized by (Y,Ce) or Ce (see next section). The formation of (Y,Ce) α′ and Ce α′ phase in the ceramics is attributed to the meta-stability of SHS-ed Ce α′ composition and the addition of Y_2O_3.

3.4. Microstructures and mechanical properties of Ce α′ materials

Fig. 3 shows SEM photograph of hot-pressed Ce1 sample in the back-scattered mode and the corresponding EDS spectra of α′ phase and grain boundary. It can be seen from Fig. 3 (a) that there are three kinds of colors in SEM photo, i.e. dark, gray and white, corresponding

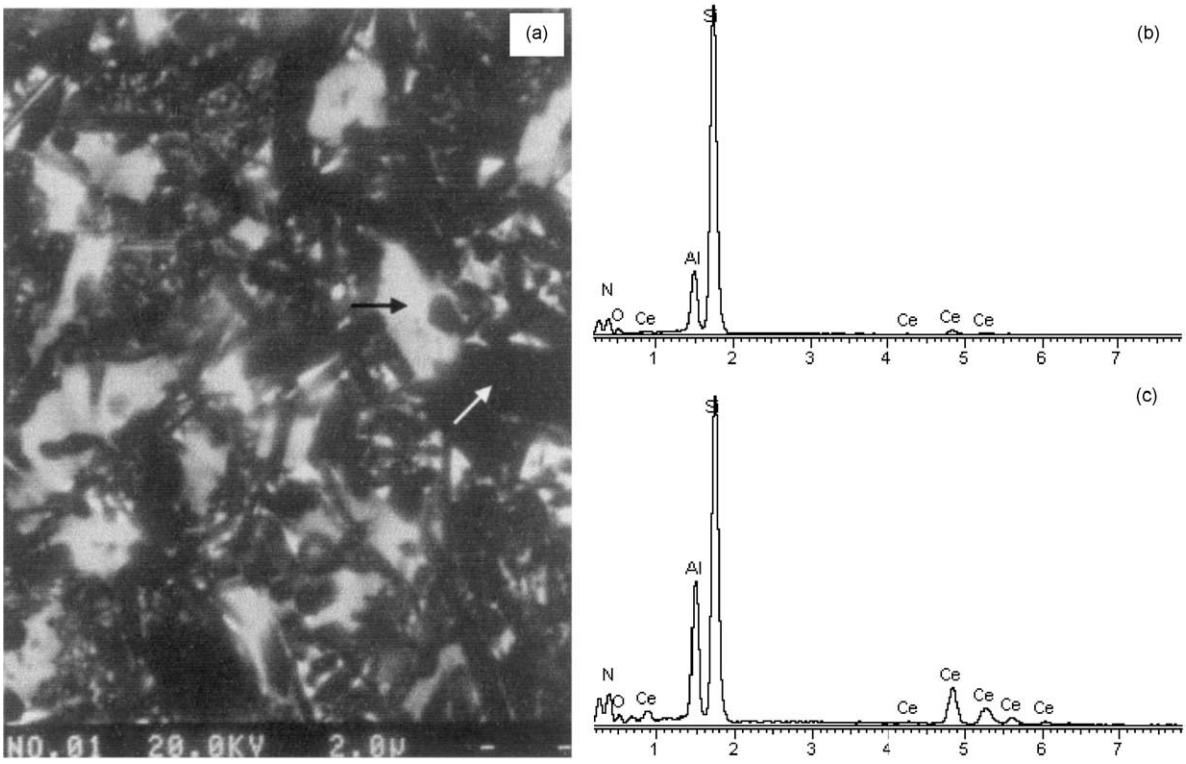

Fig. 3. (a) Backscattered SEM photograph of hot-pressed Ce1 sample (b) EDS spectrum of α′ grains (c) EDS spectrum of grain boundary phase (marked by arrows).

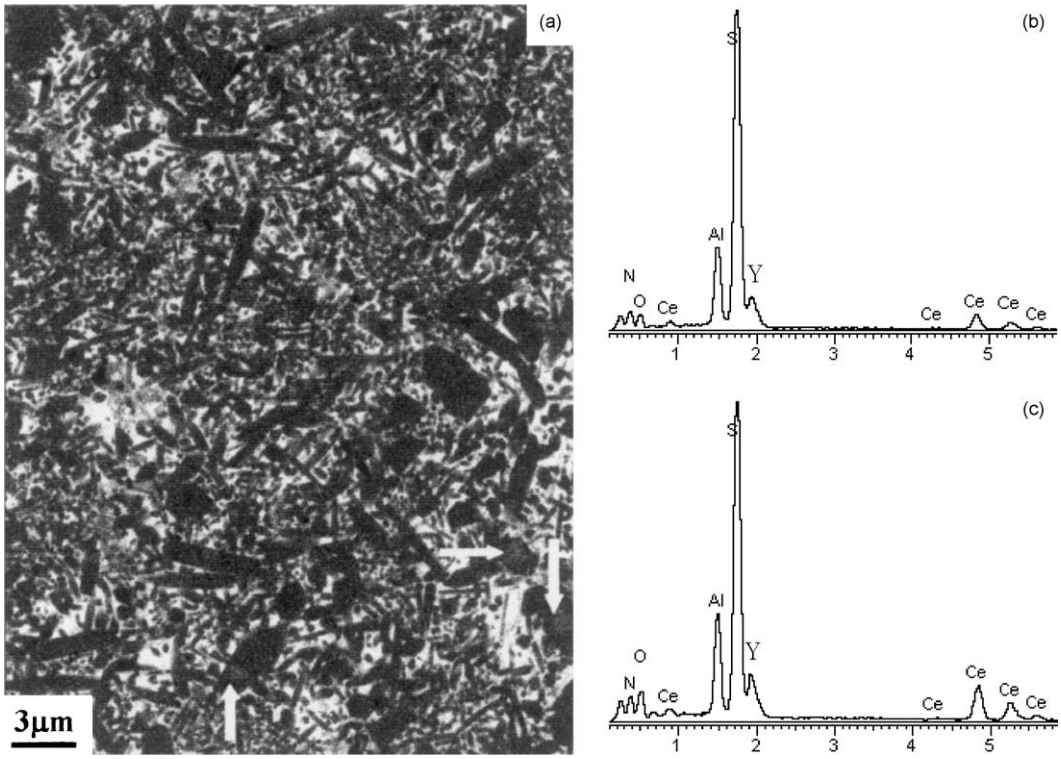

Fig. 4. (a) SEM photograph of Ce8Y3 sample (grains marked by white arrows are those with the core–edge structure) (b) EDS spectrum of α′ grains (c) EDS spectrum of grain boundary phase.

Table 3
Mechanical property of Ce α′ samples derived from SHS powder with addition of Y_2O_3

Sample	Phase assemblages[a]	H_v (GPa)	K_{1C} (MPa·m$^{1/2}$)
Ce1	β′/s, JEM/mw, α′/w	15.05	5.14
Ce8Y1	β′/s, α′/m, JEM/w	15.33	4.33
Ce8Y2	α′/s, β′/ms, M′/m	15.09	4.65
Ce8Y3	α′/s, M′/mw	15.23	4.90

[a] α′ = α-Sialon; β′ = β-Sialon; M′ = melilite solidation phase; JEM = $Ce(Si_{6-z}Al_z)(N_{10-z}O_z)$; $z \approx 1$; s = strong; ms = medium strong; m = medium; mw = medium weak; w = weak.

to β′, α′ and grain boundary phase respectively because of no or different amount of Re^{3+} ions included. Most of β′ grains are elongated or even needle-like. α′ grains with both elongated and equi-axed morphologies were observed.

Fig. 4(a) is SEM photograph of Ce8Y3 sample (back scattered mode) and the corresponding EDS spectra of α′ grains and grain boundary. It is noted that elongated is a dominant morphology of α′ grains in Ce8Y3 sample. As shown in Fig. 4(a) that there are some grains with the core–shell structure (marked by arrows) and the core is light than the shell, implying that core contains more Ce^{3+} than that of the shell. The core–shell structure of α′ grains in sintered sample would be attributed to the starting material, SHS-ed Ce α′ phase, although its amount in SHS-ed powders is only around 16% in comparison to β′ phase according to XRD analysis listed in Table 2. During sintering process, dissolution of Ce^{3+} from α′ into liquid phase and incorporated Y^{3+} into α′ grain would cause the unhomogenous distribution of cations in the α′ grains. As a result, more amount of Ce^{3+} could remain in the center of the α′ grains and form a possible core–shell structure. According to EDS pattern of α′ grains, as shown in Fig. 4(b), both Y and Ce were absorbed into α′ structure with the atomic ratio of Y:Ce being more than 1. It was also found during the microstructure observation of Ce8Y3 sample by back scattered mode that three kinds of colors, gray, light gray (see a black arrow) and white, appeared together in part of one SEM photo, shown in Fig. 5(a). Carefully searching the whole surface of the Ce8Y3 sample by SEM, we found there was a small area dominated by light gray in back scattered mode [Fig. 5(b), encircled by a ellipse]. Its magnified photo is shown in Fig. 5(c). EDS analysis illustrated that the α′ phase was solely stabilized by Ce ions [Fig. 5(d)]. This phenomenon might be caused by ununiformity in the mixing of starting material and revealed the possible formation of Ce α′ phase stabilized by Ce alone, not co-existing with Y in α′ grains as most α′ grains did in Ce8Y3 sample. Different from homogenous distribution of cations as usually α′ grains do have, which can be confirmed by color of SEM photo in back scattered mode, it was noted that there were some small gray points within each light gray region. The reason for appearance of small gray points, attributed to the contribution of (Y/Ce) or Y α′ phase, was unclear.

The mechanical properties of sintered Ce α′ materials are listed in Table 3. It is noted that Ce1 has the lowest hardness (15.05 GPa) and the highest toughness (5.14 MPam$^{1/2}$) among all samples, whereas higher hardness (15.23 GPa) and lower toughness (4.90 MPam$^{1/2}$) are obtained in Ce8Y3 in comparison to Ce1, resulting from higher amount of β′ and α′ existing in Ce1 and Ce8Y3 respectively. The relative lower hardness in Ce8Y2 and Ce8Y3 comparing to the ordinary sample consisting of single α′ phase is attributed to the existence of the second phase. The elongated morphology of α′ grain in Ce8Y3 sample might encourage the increase in toughness and resulting in the highest toughness (4.90 MPam$^{1/2}$) among three Y-containing samples without the contribution of β′ phase. It is noted however that the difference in the mechanical properties of these samples was not obvious. It is believed that there are various factors that affect the mechanical properties of Ce α-sialon compositions, for example, the phase assemblages, microstructure, the second crystalline phase and grain boundary. As a consequence, the mechanical properties of the materials would be a combined result, in which some explanations are still not clear, for example, why did not the elongated α′ grains result in a larger increase in K_{1c}? The further work to understand the relationships between them is needed.

4. Conclusions

SHS could be a promising synthesis method for α′ doped by large rare-earth ions Ce^{3+}, which can not be incorporated into α′ structure by conventional methods. In SHS-ed Ce α′ powder, β′ is the major crystalline phase, and the minor phases are α′, $Ce_2Si_6O_3N_8$ and AlN-polytypoid. The SHS-ed Ce α′ powders are metastable because of high speed of reaction and cooling rates during synthesis.

After the sintering of SHS-ed α′ powder, part of α′ transforms to β′ with the increase in lattice parameters of Ce α′ unit cell, and JEM phase is formed as grain boundary phase. SHS-ed Ce α′ phase could be stabilized with addition of Y_2O_3 after hot-pressed. It is found that α′ phase increases with increase in the amount of Y_2O_3 added and becomes as major crystalline phase when added Y_2O_3 reaches 0.375 molar in the starting material. The grain boundary phase varies from JEM phase to M′ phase while amount of Y_2O_3 is equal to or more than 0.25 molar. Most α′ grains are stabilized by both Y and Ce ions and show elongated morphology in hot-pressed samples. The hardness (H_v) and fracture toughness (K_{1C}) of

Ce8Y3 sample are 15.23 GPa and 4.90 $MPam^{1/2}$ respectively.

The $\alpha' \rightarrow \beta'$ transformation of SHS-ed Ce α' powder inherent in the hot-pressed process and the materials with different ratios of α':β' obtained by variable amount of addition of Y_2O_3 would provide good opportunities for microstructural modification and hence property tailoring.

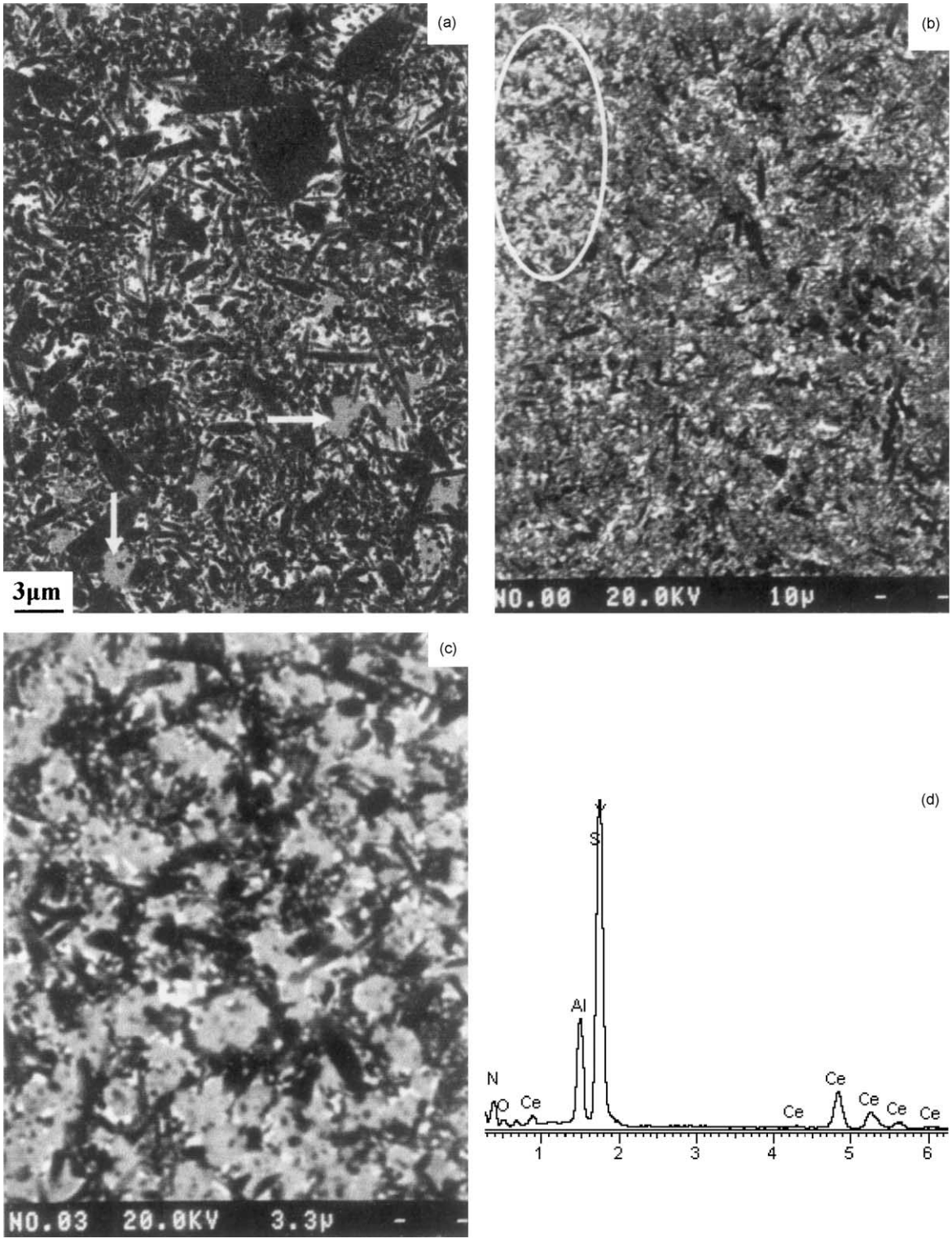

Fig. 5. (a) SEM photograph of the deep gray area (b) SEM photograph of the area containing a lighter area (encircled by a ellipse) (c) SEM photograph of the lighter area in Ce8Y3 sample (d) EDS spectrum of white-gray phase (marked by arrows).

Acknowledgements

The financial support for the research from the National Natural Science Foundation of China and the Energy Saving Investment Co. of China (No. 50272073) and the Outstanding Overseas Chinese Scholars Fund of Chinese Academy of Sciences was highly appreciated.

References

1. Ekström, T. and Nygren, M., Sialon ceramics. *J. Am. Ceram. Soc.*, 1992, **75**(2), 259–276.
2. Hampshire, S., Park, H. K., Thompson, D. P. and Jack, K. H., α-Sialon ceramic. *Nature, London*, 1978, **274**, 121–132.
3. Huang, Z. K., Tien, T. Y. and Yen, T. S., Subsolidus phase relationships in Si_3N_4–AlN–Rare-earth oxide systems. *J. Am. Ceram. Soc.*, 1986, **69**(8), C-241–C-242.
4. Söderlund, E. and Ekström, T., Pressureless sintering of Y_2O_3–CeO_2-doped Sialons. *J. Mater. Sci.*, 1990, **25**, 4815–4821.
5. Ekström, T., Jansson, K., Olsson, P. O. and Person, J., Formation of an Y/Ce-doped α-Sialon phase. *J. Eur. Ceram. Soc.*, 1991, **8**, 3–9.
6. Olsson, P. O., Crystal defects and coherent intergrowth of α- and β-crystals in Y–Ce doped Sialon materials. *J. Mater. Sci.*, 1989, **24**, 3878–3887.
7. Mandal, H., Thompson, D. P. and Ekström, T., α↔β-Sialon transformation in heat-treated Sialon ceramics. *J. Eur. Ceram. Soc.*, 1993, **12**, 421–429.
8. Rosenflanz, A. and Chen, I. W., Phase relationship and stability of α-Sialon. *J. Am. Ceram. Soc.*, 1999, **82**, 1025–1036.
9. Shen, Z. and Nygren, M., Nd-doped α-Sialon and related phase: stability and compatibility. *Mater. Sci. Forum.*, 2000, **325–326**, 191–198.
10. Wang, C. M., Mitomo, M., Xu, F. F., Hirosaki, N. and Bando, Y., Synthesis of Cerium α-Sialon with nuclei addition. *J. Am. Ceram. Soc.*, 2001, **84**(6), 1389–1391.
11. Shen, Z. and Nygren, M., Implications of kinetically promoted formation of metastable α-Sialon phases. *J. Eur. Ceram. Soc.*, 2001, **21**, 611–615.
12. Yi, H. C. and Moore, J. J., Review: self-propagating high-temperature (combustion) synthesis (SHS) of powder-compacted materials. *J. Mater. Sci.*, 1990, **25**, 1159–1168.
13. Jiang, G. J., Zhuang, H. R., Li, W. L., Wu, F. Y., Zhang, B. L. and Fu, X. R., Mechanisms of combustion synthesis of Aluminum Nitride in high pressure nitrogen atmosphere (2). *J. Mater. Synth. Process.*, 1999, **7**, 1–6.
14. Chen, K. X., Jin, H. B., Zhou, H. P. and Ferreira, J. M. F., Combustion synthesis of AlN-SiC solid solution particles. *J. Eur. Ceram. Soc.*, 2000, **20**, 2601–2606.
15. Chen, W. W., Wang, P. L., Chen, D. Y., Zhang, B. L., Jiang, J. X., Cheng, Y. B. and Yan, D. S., Synthesis of (Ca,Mg)-α-Sialon from slag by self-propagating high-temperature synthesis. *J. Mater. Chem.*, 2002, **12**, 1199–1202.
16. Jiang, J. X., Wang, P. L., Chen, W. W., Zhuang, H. R., Cheng, Y. B. and Yan, D. S., Study on phase assemblages of (Ca,Mg)-α-Sialon ceramics starting from SHS-ed α-Sialon powder. *J. Eur. Ceram. Soc.*, 2003, **23**, 2343–2349.
17. Johansson, K. E., Palm, T. and Werner, P. E., An automatic microdensitometer for X-ray diffraction photographs. *J. Phys. E.: Sci. Instrum.*, 1980, **13**, 1289–1291.
18. Werner, P. E., A fortran program for least-squares refinement of crystal-structure cell dimensions. *Arkiv fur Kemi*, 1964, **31**, 513–516.
19. Hwang, J. C., Susnitzky, D. W. and Beaman, D. R., Preparation of multication α-Sialon containing strontium. *J. Am. Ceram. Soc.*, 1995, **78**, 588–592.
20. Hwang, J. C., Susnitzky, D. W., Newman, R. A., Beaman, D. R. and Pyzik, A. J., Controlled crystallization in self-reinforced silicon nitride with Y_2O_3, SrO and CaO: crystallization behavior. *J. Am. Ceram. Soc.*, 1995, **78**, 3072–3080.
21. Huang, Z. K., Jiang, Y. Z. and Tien, T. Y., Formation of α-Sialons with dual modifying cations (Li + Y and Ca + Y). *J. Mater. Sci. Lett.*, 1997, **16**, 747–751.